# Geometry-Aided Joint Estimation of Short Range MIMO Channels with Hybrid Transceivers

Shima Eslami, Bikshapathi Gouda, Antti Tölli and Dileep Kumar
Centre for Wireless Communications, University of Oulu, Finland
Emails: {shima.eslami, bikshapathi.gouda, antti.tolli, dileep.kumar}@oulu.fi

***Abstract*—In short-range millimeter wave (mmWave) multiple-input multiple-output (MIMO) communication scenarios the distance between transceivers is often comparable to the size of antenna arrays. The resulting line-of-sight (LoS) MIMO channel has typically a rank higher than one, and hence, conventional channel estimation methods based on the far-field approximation may not be applicable. In this paper, we consider the uplink channel estimation problem using a hybrid transceiver architecture and propose a geometry-assisted, maximum likelihood (ML)-based joint estimation of a short-range LoS channel with a reduced number of pilot transmissions. Under the near-field assumption, the proposed approach exploits the known RX geometry and describes the joint likelihood function based on the intersection of two antenna-specific reference angle of arrivals (AoAs). Relying on limited subarray-specific pilot measurements, all antenna-specific AoAs and subarray-specific correction factors can be computed using geometry dependencies among estimated reference AoAs, which in turn can be used for channel reconstruction. Simulation results show that the proposed method is able to reliably estimate the short range MIMO channel with a greatly reduced number of measurements compared to the previous works.**

## I. Introduction

Millimeter wave multiple-input multiple-output (mmWave-MIMO) systems are well known for offering the capability of packing a large number of antennas in small devices (e.g., wearables), which enables highly directional communication links [1]. On the other hand, to reduce the implementation cost and power consumption of a large number of antenna elements in mmWave-MIMO transceivers, hybrid beamforming architecture are often used in practice [2].

Channel estimation is crucial for a beamforming system to achieve high data rates. Due to the limited number of RF chains in hybrid beamforming systems, conventional channel estimation methods typically require a large number of measurements across distinct analog beamformer configurations in time domain [3]. To tackle this challenge, prior works have proposed different methods based on the sparsity and low-rank property of the mmWave channel matrix [3]–[6]. Most of these methods are based on the far-field assumption, which is not necessarily applicable to the short-range line-of-sight (SR-LoS) channels where the distance between the transceivers is comparable to antenna array dimensions, and the rank of the channel matrix can be much larger than one [7].

Prior works on the SR-LoS scenarios have proposed a message passing (MP)-based channel estimation method in which the MIMO channel is split into several subchannels, and the far-field approximation is applied to each subchannel separately [8]–[10]. In these works, the MIMO channel was characterized by the local angle-of-arrivals (AoAs) defined for each subarray of the RX array. The MP algorithm was performed utilizing the geometry dependencies among the local AoAs. However, the MP methods proposed in [8], [9] require supplementary knowledge of the distance uncertainty range between the transceivers, which can significantly limit the estimation performance if the actual TX-RX distance falls beyond the uncertainty range. Furthermore, the knowledge of the RX geometry has not been fully exploited in [8]–[10] as the geometry knowledge allows for modeling more precise antenna-specific channels. For short distances, even the far-field approximation for each sub-channel/array does not hold anymore. Near field channel estimation and channel modeling have been studied in literature such as [11]–[13]. However, the geometry information has not been exploited in these works.

In this paper, we propose a geometry-assisted, maximum likelihood (ML)-based joint estimation (over the entire array of sub-arrays) method to estimate an SR-LoS MIMO channel. Our framework assumes a subarray-based hybrid beamforming system at the RX and a fully digital architecture at the TX[1]. We consider the near-field assumption, meaning that unlike [8]–[10], the MIMO channel is characterized by the antenna-specific AoAs instead of subarray-specific AoAs. By leveraging the geometry dependencies among AoAs, we construct the joint likelihood function based on the intersection of two reference AoAs (two outermost AoAs) to form a two-dimensional search space and, after aggregating all parallel subarray-specific measurements acquired at the output of distinct (semi-random) analog RX beamformer configurations, provide a joint ML estimation framework with low computational complexity. Using the estimated reference AoAs along with the known RX geometry and the estimated subarray-specific correction factors, all antenna-specific AoAs are computed given the estimated TX antenna locations and consequently used to reconstruct the LoS MIMO channel. We also apply our scheme to the case where the far-field is assumed to hold for each subchannel

This work is supported by the Academy of Finland under grants no. 346208 (6G Flagship) and 343586 (CAMAIDE).

[1]Extension to hybrid beamforming-based transmitter can be implemented similarly to [9].

(subarray), similarly to [8]–[10]. In addition, we modify the original MP-based schemes [8]–[10] to include the proposed subarray-specific phase correction factor estimation method and use it as an additional reference case. Simulation results demonstrate that the proposed joint estimation method can provide much better accuracy and a greater achievable rate than the reference cases.

## II. System Model and Problem Formulation

We consider a point-to-point mmWave MIMO system in which both the TX and RX consist of $N_{\mathrm{RF}}$ RF chains (see Fig. 1). Each RF chain at the RX is connected to $N$ half-wavelength spaced uniform linear array (ULA) of antennas called a subarray. Thus, the total number of RX antennas is $N_{\mathrm{RX}} = NN_{\mathrm{RF}}$. For simplicity, we assume that all RX antennas are collinear. Given the total size of the array, the spacing between the adjacent subarrays can be larger than $\frac{\lambda}{2}$, where $\lambda$ is the wavelength. Furthermore, the beamforming architecture used at the RX is assumed to be analog in each subarray, consisting of $N$ phase shifters. On the other hand, without loss of generality, the TX is equipped with the $N_{\mathrm{TX}} \triangleq N_{\mathrm{RF}}$ antennas with fully digital beamforming architecture with arbitrary spacing between adjacent TX antennas. Let $L_{\mathrm{TX}}$ and $L_{\mathrm{RX}}$ denote the physical length of the TX and the RX arrays, respectively. Also, $d$ indicates the distance between the midpoint of the TX and RX arrays. Additionally, we use $\gamma$ and $\psi$ angles to denote the orientation of the TX array relative to the normal of the RX array and the horizontal plane, respectively.

Let $\mathbf{H} \in \mathbb{C}^{N_{\mathrm{RX}} \times N_{\mathrm{TX}}}$ denote the MIMO channel, which is assumed to be narrowband for simplicity. Then, the $(i,j)^{th}$ entry of the channel matrix is given by

$$h(i,j) = \beta_{ij}\, exp\left(\frac{-\mathrm{j}2\pi d_{ij}}{\lambda}\right), \forall i \in \mathcal{I}_{NN_{\mathrm{RF}}}, \forall j \in \mathcal{I}_{N_{\mathrm{RF}}} \quad (1)$$

where $\beta_{ij}$ and $d_{ij}$ are the path attenuation and the distance between the $i^{th}$ RX antenna and the $j^{th}$ TX antenna, respectively, and the set $\mathcal{I}_X = \{1, ..., X\}$. The path attenuation is defined as $\beta_{i,j} = (\frac{\lambda}{4\pi d_{ij}})^{\eta}$, where $\eta$ is the path-loss exponent. The channel matrix can be split as $\mathbf{H} \triangleq [\mathbf{h}_1, \ldots, \mathbf{h}_{N_{\mathrm{RF}}}]$, where $\mathbf{h}_j \in \mathbb{C}^{N_{RX}}$ is the channel vector between the RX array and the $j^{th}$ TX antenna. To denote the subarray-specific channels, i.e., subchannels, we further represent each column of $\mathbf{H}$ as $\mathbf{h}_j \triangleq [\mathbf{h}_{1,j}^{\mathrm{T}}, \ldots, \mathbf{h}_{N_{\mathrm{RF}},j}^{\mathrm{T}}]^{\mathrm{T}}$, where $\mathbf{h}_{k,j}$ is the channel between the $k^{th}$ RX subarray and $j^{th}$ TX antenna. As in SR-LoS scenarios, the rank of $\mathbf{H}$ can be greater than one, channel estimation based on the far-field assumption may perform poorly. In this paper, we aim to model and estimate the channel matrix $\mathbf{H}$ using the near-field assumption. We also discuss a scenario similar to [8]–[10] in which the far-field assumption holds for each subchannel. In this situation, each subchannel can be modeled according to a geometric parameter specific to the associated subarray. In the remainder of the paper, we refer to this setup as the subarray-specific modeling case.

### A. Pilot Transmission and Channel Measurements

We use $\mathbf{t}_j[m] \in \mathbb{C}^L$ to denote the pilot with length $L$, transmitted by the $j^{th}$ TX antenna at the $m^{th}$ training slot. Let $\mathbf{w}_k[m] \in \mathbb{C}^N$ be the receiver beam training vector used by the $k^{th}$ RX subarray during the $m^{th}$ training slot to acquire the channel measurement $\tilde{\mathbf{y}}_k[m] \in \mathbb{C}^{1\times L}$ as

$$\tilde{\mathbf{y}}_k[m] = \mathbf{w}_k^{\mathrm{H}}[m] \sum_{j=1}^{N_{RF}} \mathbf{h}_{k,j}\sqrt{\rho_j}\, \mathbf{t}_j^{\mathrm{H}}[m] + \tilde{\mathbf{n}}_k^T[m], k \in \mathcal{I}_{N_{\mathrm{RF}}} \quad (2)$$

where $\rho_j$ is the transmit power of the $j^{th}$ TX antenna, and $\tilde{\mathbf{n}}_k[m] \sim \mathcal{CN}(\mathbf{0}, \sigma^2\mathbf{I}_L)$. Without loss of generality, let us consider a scenario in which all TX antennas transmit normalized orthogonal pilots during each training slot. Under these circumstances, we can process the channel measurement of the TX antennas individually. Let us now focus on the channel measurements associated with the first TX antenna. Thus, after decorrelating with the pilot sequences, (2) is simplified to

$$y_k[m] = \sqrt{\rho_1}\, \mathbf{w}_k^{\mathrm{H}}[m]\, \mathbf{h}_{k,1} + n_k[m], \ \forall k \in \mathcal{I}_{N_{RF}}, \quad (3)$$

where $y_k[m] = \tilde{\mathbf{y}}_k[m]\mathbf{t}_1[m]$ and $n_k[m] = \tilde{\mathbf{n}}_k[m]\mathbf{t}_1[m]$. Similarly to [8]–[10], we use shifted Zadoff-Chu (ZC) sequences for the semi-random RX beam training vectors due to their advantageous properties, such as constant amplitude and zero autocorrelation. Furthermore, they can be realized in beamformers with unimodolus constraints. If $\mathbf{z}_k \in \mathbb{C}^N$ is defined as the ZC sequence corresponding to the $k^{th}$ RX subarray, the vectors $\{\mathbf{w}_k[m]\}_{m=1}^M$ are chosen as $M$ distinct random circulant shift of $\mathbf{z}_k$. Since the receiver can perform $N_{RF}$ parallel channel measurements, and there are $NN_{RF}^2$ entries in $\mathbf{H}$, the training overhead of the conventional channel estimation based on the exhaustive search requires $NN_{RF}$ training slots. This paper proposes a geometry-based channel estimation performed by transmitting far fewer than $NN_{RF}$ pilots. We will also see that for an appropriate approximation of the channel attenuation,the MIMO channel matrix can be reconstructed with a single pilot transmission per TX antenna.

## III. Geometry-Aided Joint AoA Estimation

In this section, we describe the joint channel estimation algorithm based on the known geometry of the receiver. According to (1), the LoS MIMO channel depends on the antenna-specific distances and attenuations. Hence, we define $r_{i,k}$ and $\alpha_{i,k}$ as the distance and the complex gain corresponding to the channel coefficient between the first TX antenna and the $i^{th}$ antenna element at the $k^{th}$ RX subarray. The $k^{th}$ subchannel can be then split in two parts as

$$\mathbf{h}_{k,1} \simeq \boldsymbol{\alpha}_k(r_{1,k}, ..., r_{N,k}) \odot \mathbf{a}_k(r_{1,k}, ..., r_{N,k}), \forall k \in \mathcal{I}_{N_{\mathrm{RF}}} \quad (4)$$

where $\boldsymbol{\alpha}_k \triangleq [\alpha_{1,k}, ..., \alpha_{N,k}]^T$ is a complex-valued vector, which includes relative amplitude difference among antennas as well as possible phase correction factors to compensate for the mismatch (e.g. due to a finite grid in Algorithm 1) between the actual measurements and approximated channel components (cf. Section III-B). The vector $\mathbf{a}_k(r_{1,k}, ..., r_{N,k}) \triangleq$

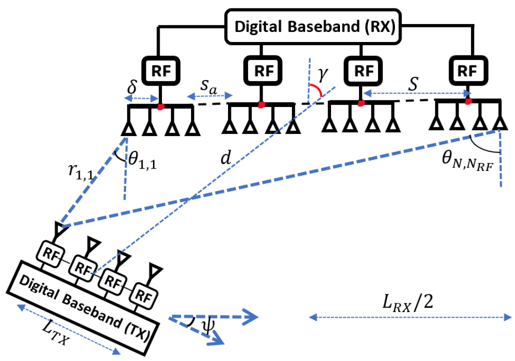


Fig. 1: A short-range LoS MIMO setup with $N_{RF} = 4$, $N = 4$, and $N_{TX} = 4$, the angle of arrival and the distances are antenna-specific because of the near field assumption.

$\left[e^{-\mathrm{j}2\pi r_{1,k}/\lambda}, ..., e^{-\mathrm{j}2\pi r_{N,k}/\lambda}\right]^T$ is the general array response vector in the $k^{th}$ subchannel which contains phases only. In general, without exploiting the underlying geometry, an exhaustive search must be performed over all possible values of antenna-specific distance parameters. At the same time, due to the small wavelength, the distance search space must have a very fine (sub-wavelength) granularity to provide an accurate estimation. To this end, we introduce the antenna-specific AoA $\theta_{i,k}$ as the angle made by the ray between the TX antenna (TX antenna index omitted for simplicity) and the $i^{th}$ antenna element of the $k^{th}$ subarray. By leveraging the knowledge of the RX geometry, which is assumed to be available at the receiver, the array response vectors in all subarrays can be represented as a function of a reference distance and AoA. In the following, we show that the reference distance can be further expressed as an intersection of two reference angles. Thus, the dimension of the search space reduces to two.

For the simplified subarray-specific modeling scenario, similar to [8], [9], we can use Vandermonde vectors as the array response vectors in each subarray. In this case, we define the subarray-specific AoAs i.e, $\theta_k$ as the angle made by the ray between the first TX antenna and the midpoint of the $k^{th}$ subarray. Therefore, the $k^{th}$ subchannel approximation can be simplified as $\mathbf{h}_{k,1} \simeq \alpha_k \mathbf{v}_k(\theta_k)$, where $\alpha_k$ is the common complex gain for all antenna elements at the $k^{th}$ subarray, and $\mathbf{v}_k(\theta_k) = \left[1, e^{-j\pi sin(\theta_k)}, \ldots, e^{-j(N-1)\pi sin(\theta_k)}\right]^T$ is the Vandermonde vector of the $k^{th}$ subarray. Similar to the general case we can leverage the geometry dependencies among the subarray-specific AoAs to reduce the overhead of the searching process. Next, we present the geometry-aided subchannel approximation and explain the steps of the joint likelihood construction.

### *A. Reformulating Array Response Vectors Using Geometry*

In this section we rewrite $\{\{r_{i,k}\}_{i=1}^{N}\}_{k=1}^{N_{RF}}$ as functions of two reference angles. It can bee seen from Figure 1 that for a given $\theta_{1,1}$, $r_{1,1}$, we can write:

$$r_{i,k} = \sqrt{(r_{1,1}\cos\theta_{1,1})^2 + (\zeta_{i,k} + r_{1,1}\sin\theta_{1,1})^2} \quad \forall k \in \mathcal{I}_{N_{RF}}, \forall i \in \mathcal{I}_N, \tag{5}$$

where $\zeta_{i,k}$ is the spacing between the first antenna of the first RX subarray and the $i^{th}$ antenna of the $k^{th}$ RX subarray, and is given by

$$\zeta_{i,k} = \big((k-1)(N-1) + (i-1)\big)\delta + (k-1)s_a, \tag{6}$$

where $\delta$ is the spacing between successive elements at each RX subarray, and $s_a$ is the spacing between the consecutive RX subarrays. Substituting (5) in the array response vector expression, we note that $\mathbf{a}_k(r_{1,k}, ..., r_{N,k}) = \mathbf{a}_k(r_{1,1}, \theta_{1,1})$. Similarly, we can obtain an expression for the AoAs as

$$\theta_{i,k} = \tan^{-1}\left(\frac{\zeta_{i,k} + r_{1,1}\sin\theta_{1,1}}{r_{1,1}\cos\theta_{1,1}}\right), \forall i \in \mathcal{I}_N, \forall k \in \mathcal{I}_{N_{\mathrm{RF}}}. \tag{7}$$

By setting $i = N$ and $k = N_{RF}$ in (7), the reference distance, can be given by

$$r_{1,1} = \frac{\zeta_{N,N_{RF}}}{(\tan\theta_{N,N_{RF}})(\cos\theta_{1,1}) - \sin\theta_{1,1}}. \tag{8}$$

It is evident that the reference distance is a function of $\theta_{1,1}$ and $\theta_{N,N_{RF}}$. Thus, $\mathbf{a}_k(r_{1,1}, \theta_{1,1}) = \mathbf{a}_k(\theta_{1,1}, \theta_{N,N_{RF}})$. In other words, $\theta_{N,N_{RF}}$ can be considered as the second reference angle. By eliminating the first index of (5), (7), and (8), and setting $\zeta_k = (k-1)s$, the expressions of $r_k$, $\theta_k$, and $r_1$ for the simplified subarray-specific modeling scenario are obtained respectively. It should be noted that $r_k$ denotes the distance between the first TX antenna and the midpoint of the $k^{th}$ RX subarray, and $s$ is the spacing between the subsequent RX subarrays. Finally, we conclude that the Vandermonde vectors are rewritten as a function of two reference angles as well, i.e., $\mathbf{v}_k(\theta_k) = \mathbf{v}_k(\theta_1, \theta_{N_{RF}}), \forall k = 2, \ldots, N_{RF} - 1$.

### *B. Computation of Vector $\boldsymbol{\alpha}_k$*

In this section, we consider two scenarios for computing vector $\boldsymbol{\alpha}_k$ In the first scenario, we simply approximate the real-valued $\beta_{i,j}$ in (1) based on the presumed path-loss model and a given $r_{i,k}$ candidate. In the second scenario, we aim to obtain an estimated value for complex vector $\boldsymbol{\alpha}_k$ based on the collected channel measurement. In the following, we discuss each scenario in more detail.

#### *1) Simple Pathloss-Based Computation (PLB-$\boldsymbol{\alpha}_k$)*

Here we assume that an approximated path-loss exponent, i.e., $\hat{\eta}$ is available and a real-valued $\alpha_{i,k}$ can be given by

$$\alpha_{i,k} = \left(\frac{\lambda}{4\pi r_{i,k}}\right)^{\hat{\eta}}, \ \forall k \in \mathcal{I}_{N_{RF}}, \forall i \in \mathcal{I}_N. \tag{9}$$

In the ideal case, $\hat{\eta} = \eta$ and $r_{i,k} = d_{i,k}$ and then $\alpha_{i,k} = \beta_{i,k}$ In practice, the angle grid granularity is finite, causing significant approximation error to reduce the estimation accuracy. Removing index $i$ from (9) gives the expression of $\alpha_k$ for the subarray-specific modeling scenario.

#### *2) Measurement-Based Computation (MB-$\boldsymbol{\alpha}_k$)*

Here, we aim to estimate the complex vector $\boldsymbol{\alpha}_k$ from channel measurements in a way that can also compensate for the phase and amplitude mismatch caused by limited angle search space. As the channel measurements are subarray-specific, we must approximate $\alpha_{i,k} \approx \alpha_k, \forall i \in \mathcal{I}_N$. We also define $\tilde{\mathbf{a}}_k(.) \triangleq \boldsymbol{\alpha}_k \odot \mathbf{a}_k(.)$ as the hypothesis vector and then aggregate

$$p(\mathbf{y}_k|\alpha_k,\theta_{1,1},\theta_{N,N_{RF}}) \propto \exp\left(\frac{-\left\|\mathbf{y}_k-\alpha_k\mathbf{W}_k^{\mathrm{H}}\mathbf{a}_k(\theta_{1,1},\theta_{N,N_{RF}})\right\|^2}{\sigma^2}\right), \forall k \in \mathcal{I}_{N_{RF}}. \tag{12}$$

all $M$ measurements in (3) to write the resulting measurement vector approximately as

$$\mathbf{y}_k \approx \mathbf{W}_k^{\mathrm{H}}\,\tilde{\mathbf{a}}_k(\theta_{1,1},\theta_{N,N_{RF}})+\mathbf{n}_k,\ \forall k \in \mathcal{I}_{N_{RF}}, \tag{10}$$

where, the $m^{th}$ entry of $\mathbf{n}_k$ is $n_k[m]$, and $m^{th}$ column of $\mathbf{W}_k$ is $\mathbf{W}_k(:,m)=\sqrt{\rho_1}\mathbf{w}_k[m]$. It is evident from (10) that for a fixed $\theta_{1,1}$, $\theta_{N,N_{RF}}$, and $\alpha_k$ the measurement vector $\mathbf{y}_k$ is a realization of $\mathcal{N}_c(\mathbf{W}_k^{\mathrm{H}}\,\tilde{\mathbf{a}}_k(\theta_{1,1},\theta_{N,N_{RF}}),\sigma^2\mathbf{I})$. Thus, the optimization problem to minimize the mismatch between the hypothesis vector and the actual measurements is given by

$$\underset{\alpha_k\in\mathbb{C}}{\text{maximize}}\ \ p(\mathbf{y}_k|\alpha_k,\theta_{1,1},\theta_{N,N_{RF}}), \tag{11}$$

where the objective function is given in (12), and $p(.)$ denotes the probability density function (PDF). By taking the derivative of the objective function with respect to $\alpha_k$ and setting it to zero, we obtain

$$\alpha_k=\frac{\left(\mathbf{W}_k^{\mathrm{H}}\mathbf{a}_k(\theta_{1,1},\theta_{N,N_{RF}})\right)^{\mathrm{H}}\mathbf{y}_k}{\|\mathbf{W}_k^{\mathrm{H}}\mathbf{a}_k(\theta_{1,1},\theta_{N,N_{RF}})\|^2},\ \forall k \in \mathcal{I}_{N_{RF}}. \tag{13}$$

The corresponding measurement-based $\alpha_k$ for the subarray-specific modelling case is obtained by replacing $\mathbf{a}_k(\theta_{1,1},\theta_{N,N_{RF}})$ with $\mathbf{v}_k(\theta_1,\theta_{N_{RF}})$ in (12) and (13). It is seen that the complex gain parameter is always a function of the associated reference angles.

### *C. Joint Likelihood Construction*

Now, we can define the joint likelihood function by collecting the measurement vectors of all RX subarrays as

$$p(\mathbf{y}_1,\ldots,\mathbf{y}_{N_{RF}}|\theta_{1,1},\theta_{N,N_{RF}})=\prod_{k=1}^{N_{RF}}p(\mathbf{y}_k|\theta_{1,1},\theta_{N,N_{RF}}), \tag{14}$$

which can also be represented in an extended form shown in (15) (top of the next page). Similarly, the joint likelihood function for the simplified subarray-specific alternative is obtained by defining $\tilde{\mathbf{v}}_k(.)\triangleq\alpha_k\mathbf{v}_k(.)$ and removing the first index from the reference AoAs in (15).

### *D. Joint Estimation Algorithm*

Having computed the joint likelihood function, the search process can be started. Our joint estimation method is based on evaluating the joint likelihood function over a two-dimensional angle search space and choosing the best pair for the reference angles. In other words, the most likely values for $\theta_{1,1}$ and $\theta_{N,N_{RF}}$ can be described as

$$(\hat{\theta}_{1,1},\hat{\theta}_{N,N_{RF}})=\underset{\{\theta_{1,1},\theta_{N,N_{RF}}\}}{\text{argmax}}\ p(\mathbf{y}_1,\ldots,\mathbf{y}_{N_{RF}}|\theta_{1,1},\theta_{N,N_{RF}}). \tag{16}$$

The distances and AoAs for all other antenna pairs can be computed from (5) and (7) , respectively. Similar expression can be given for the $(\hat{\theta}_1,\hat{\theta}_{N_{RF}})$ by removing the first index from AoAs in (16).

It should be noted that due to the geometry dependencies of the AoAs, all intersections of two reference angles are not feasible. It means that the search overhead can be reduced by considering only the feasible intersections during the search process. For example, all intersections resulting in a negative $r_{1,1}$ are infeasible by default. Also, if there is a prior knowledge of the feasible distance range, and the computed $r_{1,1}$ does not lie within the range, the corresponding angle pairs can be excluded from the search space. The proposed geometry-aided joint estimation method is summarized in Algorithm 1. The flow of the algorithm for the simplified subarray-specific modeling case is similar, only the antenna-specific indices are replaced with subarray-specific indices.

### *E. Channel Reconstruction and Achievable Rate Computation*

To reconstruct the LoS MIMO channel matrix, we can estimate the location of the TX array and compute the distance between each TX-RX antenna. To this end, similar to [8], we define $\mathbf{p}=(\mathbf{p}_1-\mathbf{p}_{N_{RX}})/\|\mathbf{p}_1-\mathbf{p}_{N_{RX}}\|_2$ as a unit vector along the RX array, where $\mathbf{p}_1$ and $\mathbf{p}_{N_{RX}}$ are the position vector of the first and last RX antennas. Noting the fact that the geometry of the RX antennas is available at the receiver, the position vector of all RX antennas can be easily computed at the RX. Then $\mathbf{p}$ is rotated by $\pi/2-\theta_{1,1}$ to find the direction of the first TX antenna relative to the RX array. Therefore, the estimated position vector of the first TX antenna is obtained as

$$\mathbf{q}_1=\mathbf{p}_1+\hat{r}_{1,1}\mathbf{R}(\pi/2-\hat{\theta}_{1,1})\mathbf{p}, \tag{17}$$

where $\mathbf{R}(\omega)$ is the rotation matrix with the angle $\omega$ and is given by

$$\mathbf{R}(\omega)=\begin{bmatrix}\cos(\omega) & -\sin(\omega)\\ \sin(\omega) & \cos(\omega)\end{bmatrix}. \tag{18}$$

It should be noted that for the simplified subarray-specific modeling case, we have $\mathbf{q}_1=\mathbf{s}_1+\hat{r}_1\mathbf{R}(\pi/2-\hat{\theta}_1)\mathbf{p}$, where $\mathbf{s}_1$ is the position vector of the first RX subarray. Similarly, by applying Algorithm 1 to the channel measurements of the last TX antenna, we can find its position vector, i.e., $\mathbf{q}_{N_{RF}}$ as described above for $\mathbf{q}_1$. Finally, the position vectors of the rest TX antennas are acquired using $\mathbf{q}_1$, $\mathbf{q}_{N_{RF}}$, and the known TX geometry. It is worth noting that the problem of estimating the TX location using the estimated AoAs is similar to a localization problem. Investigating the application of our approach in localization scenarios is an interesting direction for future work. Having estimated the MIMO channel, the precoder and the combiner matrices can be designed. By computing the singular value decomposition of the estimated channel, i.e., $\hat{\mathbf{H}}=\hat{\mathbf{U}}\hat{\mathbf{\Sigma}}\hat{\mathbf{V}}^{\mathrm{H}}$, we can use the singular matrices $\hat{\mathbf{U}}$ and $\hat{\mathbf{V}}$ as the combiner and the precoder at the RX and TX, respectively. The achievable rate of our setup is computed from the capacity of MIMO channel $\hat{\mathbf{U}}^{\mathrm{H}}\mathbf{H}\hat{\mathbf{V}}$.

$$p(\mathbf{y}_1,\ldots,\mathbf{y}_{N_{RF}}|\theta_{1,1},\theta_{N,N_{RF}}) \propto \exp\Bigg(\sum_{k=1}^{N_{RF}} \frac{-\|\mathbf{y}_k-\mathbf{W}_k\tilde{\mathbf{a}}_k(\theta_{1,1},\theta_{N,N_{RF}})\|^2}{\sigma^2}\Bigg). \quad (15)$$

**Algorithm 1** Joint Estimation Algorithm

**Data:** Collected measurements $\{\mathbf{y}_k\}_{k=1}^{N_{RF}}$, RX beam training matrices $\{\mathbf{W}_k\}_{k=1}^{N_{RF}}$, noise variance $\sigma^2$, Prior distance information $r_{min}$ and $r_{max}$ (if available), resolution of the angle search space $\Delta\theta$, and the RX array geometry information.
**Initialization:** set the initial values of the joint likelihood to zeros.

```
while θ_{1,1} ≤ θ_max do
    θ_{N,N_RF} = θ_min
    while θ_{N,N_RF} ≤ θ_max do
        Compute r_{1,1} using (8).
        if (r_{1,1} ≥ r_min) and (r_{1,1} ≤ r_max)
            Compute a_k(θ_{1,1}, θ_{N,N_RF}) using (5),(6), and (8).
            Compute the elements of α_k using (9) or (13).
            Compute the joint likelihood function from (15)
        end if
        θ_{N,N_RF} = θ_{N,N_RF} + Δθ
    end
    θ_{1,1} = θ_{1,1} + Δθ
end
```

- Compute $(\hat{\theta}_{1,1},\hat{\theta}_{N,N_{RF}})$ as in (16)
- Compute $\{\{\hat{\theta}_{i,k}\}_{i=1}^{N}\}_{k=1}^{N_{RF}}$ from (7) and $\{\{\hat{r}_{i,k}\}_{i=1}^{N}\}_{k=1}^{N_{RF}}$ using (5).

## IV. Simulation Results

In this section, we evaluate the performance of our proposed approach with some numerical examples. We consider $N_{RF}=4$ subarrays at the RX with $N=32$ antennas per subarray. The carrier frequency is set to $60$ GHz, which corresponds to $\lambda=5$ mm. The spacing between adjacent RX subarrays is $s_a=1$ cm, and the length of the arrays at the TX and the RX is $L_{\text{TX}}=4$ cm and $L_{\text{RX}}=34$ cm. The respective TX-RX location is determined by the 3-tuple $(d,\gamma,\psi)$. The angle $\gamma$ is randomly chosen from $|\gamma| <= \gamma_{\max}{}^\circ$, and $\psi$ is set to $90°$. Furthermore, for Figure 2 and Figure 3, the distance $d$ is randomly selected from $[10,100]$. The reported simulation results are for 1000 different channel realizations, which correspond to 1000 random TX-RX relative locations. It is mentioned that for simplicity, the simulated channels include only the LoS components. To consider a more realistic simulation setup, we can include the NLoS components in the channel realizations similar to [7]–[10]. Although, our algorithm recovers only LoS components, the relative performance difference among the investigated cases will not be changed . Extending the algorithm to reconstruct the NLoS components is left for the future study. As a reference, we modify the MP method proposed in [10] by considering ULA at the RX and comparing it with our results. We also add the independent subarray-specific processing method as well as the exhaustive search approach both from [8] to our comparisons. All these benchmark cases assume the far-field approximation for each subchannel/subarray and estimate the channel by independently maximizing the associated likelihood of each local AoA. In addition, we modify all three aforementioned cases using MB-$\alpha$ to assess the effect of the phase correction factors on the previous works.

In Figure 2, we investigate the proposed joint estimation (JE) method for different scenarios. The following observation can be highlighted from this figure: i) The accuracy of channel estimation with the near-field assumption is superior to the subarray-specific modelling case, i.e., JE (SA). Furthermore, we observe that the proposed method can achieve a close to optimal rate performance even with $M<5$ measurements. ii) As expected, the performance of the proposed method using PLB-$\boldsymbol{\alpha}_k$ becomes degraded when the search space is limited. On the other hand, as the estimated measurement based MB-$\boldsymbol{\alpha}_k$ can compensate for the mismatch between the actual measurements and the hypothesis vector, even with the lower-resolution angle space, the accuracy of the estimation method is significantly improved. iii) Our method needs at least two channel measurements to compute MB-$\boldsymbol{\alpha}_k$ and perform the estimation. However, the JE method using PLB-$\boldsymbol{\alpha}_k$ can be performed even with one channel measurement.

Figure 3 compares the proposed JE method with various benchmark cases. It is apparent that there is a large performance gap between the proposed method and other schemes. More specifically, for $M=3$ the rate of the JE method is significantly better than the other cases. We can also observe that although the original MP method with heuristic $\alpha_k$ estimates (see [8]–[10]) does not perform particularly well in our setup with relatively coarse search granularity. However, by applying the MB-$\boldsymbol{\alpha}_k$ from (13), the rate of the MP method is considerably increased. Moreover, with increasing $M$, the performance of the improved MP and the independent subarray-specific processing (Independent SA) methods becomes almost the same as the JE with subarray-specific modeling.

Figure 4 shows the effect of the distance between the transceivers on the performance of the proposed joint estimation method compared with the existing MP and Independent SA with MB-$\alpha_k$ with 5 channel measurements. It can be observed that with a very short TX-RX distance, the JE method is significantly superior to the methods with far-field assumption per subarray. On the other hand, as $d$ increases beyond 100cm, the difference between antenna- and subarray-based methods vanishes. In general, the achievable rate with fixed SNR decreases w.r.t TX-RX distance $d$ as the far-field assumption begins to hold and channel rank is reduced. At the same time, the gap between the perfect CSI and the estimated CSI increases as the finite grid size and limited number of measurements reduce the performance of the geometry-aided methods. However, the gap can be significantly reduced with a higher search granularity.

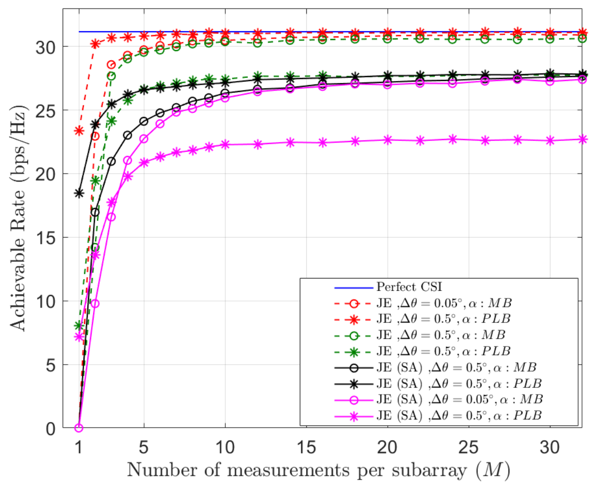


Fig. 2: Achievable rate of geometry-based joint estimation methods for an SNR of 10 dB and $\gamma_{\max} = 75^\circ$.

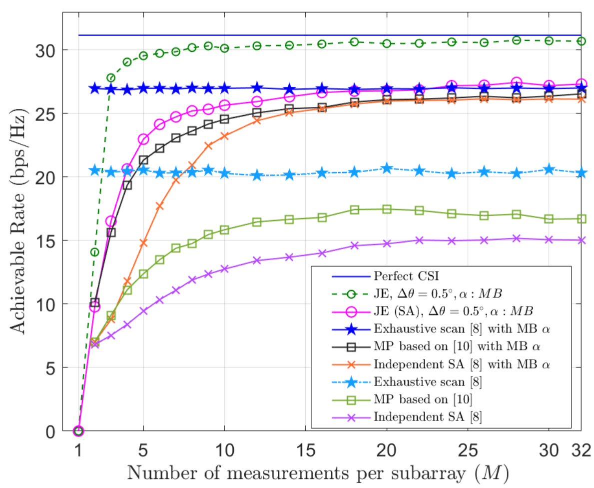


Fig. 3: Achievable rate of different estimation methods for an SNR of 10 dB and $\gamma_{\max} = 75^\circ$.

## V. Conclusions

In this paper, we proposed a low-complexity ML-based joint estimation method to estimate the MIMO channel for short-range LoS settings, such as wearables, with subarray-based hybrid beamforming architecture. Assuming a near-field scenario and leveraging the knowledge of the RX geometry, proposed joint estimation scheme is able to parameterize the MIMO channel in terms of only two antenna-specific reference AoAs. Simulation results revealed that the proposed method is able to reconstruct the MIMO channel with high accuracy with few pilot transmissions which is useful to minimize the channel measurement overhead. Moreover, the proposed method significantly outperformed the existing methods that relied on the subarray-specific far-field approximation.

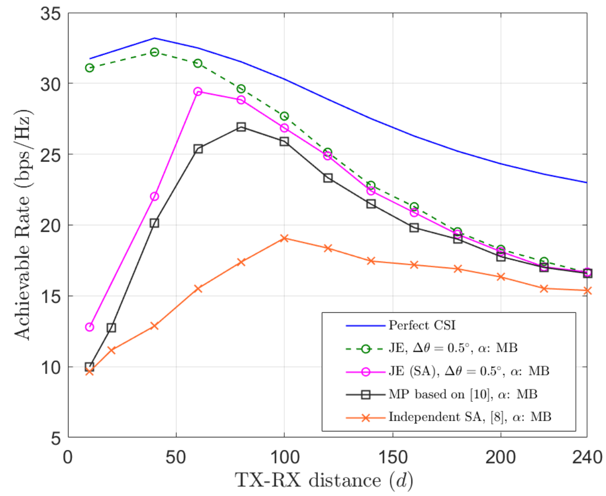


Fig. 4: Achievable rate of different estimation methods versus the relative TX-RX distance for an SNR of 10 dB, $\gamma_{\max} = 60^\circ$, and $M = 5$.

## References

[1] S. Okasaka, R. J. Weiler, W. Keusgen, A. Pudeyev, A. Maltsev, I. Karls, and K. Sakaguchi, "Proof-of-concept of a millimeter-wave integrated heterogeneous network for 5G cellular," *IEEE Sensors J.*, vol. 16, no. 9, p. 1362, Aug. 2016.

[2] T. Lin, J. Cong, Y. Zhu, J. Zhang, and K. Ben Letaief, "Hybrid beamforming for millimeter wave systems using the mmse criterion," *IEEE Trans. Commun.*, vol. 67, no. 5, pp. 3693–3708, 2019.

[3] H.-L. Chiang, T. Kadur, W. Rave, and G. Fettweis, "Low-complexity spatial channel estimation and hybrid beamforming for millimeter wave links," in *2016 IEEE 27th Annual International Symposium on Personal, Indoor, and Mobile Radio Communications (PIMRC)*, 2016, pp. 1–7.

[4] J. Rodríguez-Fernández, N. González-Prelcic, K. Venugopal, and R. W. Heath, "Frequency-domain compressive channel estimation for frequency-selective hybrid millimeter wave MIMO systems," *IEEE Trans. Wireless Commun.*, vol. 17, no. 5, pp. 2946–2960, Mar. 2018.

[5] R. W. Heath, N. González-Prelcic, S. Rangan, W. Roh, and A. M. Sayeed, "An overview of signal processing techniques for millimeter wave MIMO systems," *IEEE J. Sel. Topics Signal Process.*, vol. 10, no. 3, pp. 436–453, Feb. 2016.

[6] P. A. Eliasi, S. Rangan, and T. S. Rappaport, "Low-rank spatial channel estimation for millimeter wave cellular systems," *IEEE Transactions on Wireless Communications*, vol. 16, no. 5, pp. 2748–2759, 2017.

[7] E. Torkildson, U. Madhow, and M. Rodwell, "Indoor millimeter wave MIMO: Feasibility and performance," *IEEE Trans. Wireless Commun.*, vol. 10, no. 12, pp. 4150–4160, Oct. 2011.

[8] J. Kaleva, N. J. Myers, A. Tölli, and R. W. Heath, "A geometry-aided message passing method for AoA-based short range MIMO channel estimation," in *Proc. IEEE Int. Workshop Signal Process. Adv. in Wireless Commun. (SPAWC)*, Jul. 2019.

[9] N. J. Myers, J. Kaleva, A. Tölli, and R. W. Heath, "Message passing-based link configuration in short range millimeter wave systems," *IEEE Trans. Commun.*, vol. 68, no. 6, pp. 3465–3479, Jun. 2020.

[10] J. Kaleva, N. J. Myers, A. Tölli, R. W. Heath, and U. Madhow, "Short range 3D MIMO mmwave channel reconstruction via geometry-aided AoA estimation," in *Proc. Asilomar Conf. Signals, Syst., and Comput. (ASILOMAR)*, Nov. 2019.

[11] X. Wei and L. Dai, "Channel estimation for extremely large-scale massive mimo: Far-field, near-field, or hybrid-field?" *IEEE Communications Letters*, vol. 26, no. 1, pp. 177–181, 2022.

[12] Z. Lu, Y. Han, S. Jin, M. Matthaiou, and T. Q. S. Quek, "Near-field channel reconstruction and user localization for elaa systems," in *2022 International Symposium on Wireless Communication Systems (ISWCS)*, 2022, pp. 1–6.

[13] E. Björnson, Ö. T. Demir, and L. Sanguinetti, "A primer on near-field beamforming for arrays and reconfigurable intelligent surfaces," in *2021 55th Asilomar Conference on Signals, Systems, and Computers*. IEEE, 2021, pp. 105–112.